Title

A Separated 1.17-Bev/c K- Meson Beam

Permalink

Authors

Eberhard, Phillippe
Good, Myron L.
Ticho, Harold K.

Publication Date

1959-12-30

UCRL 8878

UNIVERSITY OF CALIFORNIA

Ernest O. Lawrence
Radiation Laboratory

BERKELEY, CALIFORNIA

To be published in R. S. I.

UCRL-8878 Rev.

UNIVERSITY OF CALIFORNIA

Lawrence Radiation Laboratory
Berkeley, California

Contract No. W-7405-eng-48

A SEPARATED 1.17-Bev/c K^- MESON BEAM

Phillippe Eberhard, Myron L. Good, and Harold K. Ticho

December 30, 1959

A SEPARATED 1.17-Bev/c K^- MESON BEAM

Phillippe Eberhard, Myron L. Good, and Harold K. Ticho

Lawrence Radiation Laboratory
University of California
Berkeley, California

December 30, 1959

Abstract

This report describes the design and testing of a 1.17-Bev/c separated K^- beam designed in the fall of 1958 in connection with a 15-in. hydrogen bubble chamber experiment. At the target the K^-/π^- ratio was 1/140. At the chamber, 4.0 K^- - meson decay lengths from the target, and after two stages of electromagnetic separation, the K^-/π^- ratio was 12.5, corresponding to a total pion suppression by a factor of about 10^5. The K^- flux at the chamber was 0.87 K^- mesons per 10^{10} protons impinging on the target.

A SEPARATED 1.17-Bev/c K^- MESON BEAM*

Phillippe Eberhard, Myron L. Good, and Harold K. Ticho†

Lawrence Radiation Laboratory
University of California
Berkeley, California

December 30, 1959

Introduction

During the fall of 1958 a beam of negative K mesons of ~1.2 Bev/c momentum was required at the Lawrence Radiation Laboratory in connection with an experiment involving the 15-in. hydrogen bubble chamber. In counting experiments it is possible to distinguish the K mesons from the much more copions pion flux by time-of-flight and Čerenkov counter techniques. Such techniques could also be used for bubble chamber research. However, the beam levels in the Bevatron ($\sim 2 \times 10^{11}$ protons per pulse) and the existing focusing equipment (8-in.-bore quadrupole lenses) are such that the number of K mesons that could be guided from target to chamber is much larger than the number the chamber can use. Under these circumstances it becomes highly advantageous to increase the target-to-chamber distance so that, while a large fraction of the K mesons decay in flight, the intervening space may be used to effect a spatial separation of the K mesons from the pion background. A beam of this character is described in the following report.

*This work was done under the auspices of the U. S. Atomic Energy Commission.

†Permanent address: Physics Department, University of California, Los Angeles.

1

In view of the fact that the momentum dispersion of beams from the Bevatron imposes symmetry about the median plane only, it seemed desirable to adopt a separation scheme in which the pions to be rejected would be deflected out of the median plane. A velocity spectrometer with a horizontal magnetic field H and a vertical electric field E has such a character. Such spectrometers, with deflection plates 230 in. long and capable of supporting ~400 kv, had recently become available at the laboratory for enriching antiproton beams.[1] When a beam of particles of momentum P and of various masses is shot into such a spectrometer, particles with velocity

$$\beta_0 = \frac{E}{H} \tag{1}$$

continue undeflected, while others suffer deflections α out of the median plane:

$$\frac{\alpha}{P_0} = \frac{\Delta}{P} \tag{2a}$$

with

$$P_0 = V\frac{\ell}{d}, \tag{2b}$$

$$\Delta = \frac{1}{\beta} - \frac{1}{\beta_0}, \tag{2c}$$

where P is the particle momentum in ev/c V is the potential applied to the plates in volts, ℓ and d are the length and separation of the plates, respectively, and Δ is the deviation of $(1/\beta)$ of the particle from $1/\beta_0$. In the relativistic domain $(p/\mu \gg 1)$, we have

$$\frac{\alpha}{P_0} \approx \frac{\mu_1^2 - \mu_0^2}{2P^3}, \tag{3}$$

where μ_0 is the mass of the particle to which Eq. (1) applies and μ_1 is the mass of the particle to be deflected. In Fig. 1, the angle α_π of pions relative to K

---

[1] Coombes, Cork, Galbraith, Lambertson, and Wenzel, Phys. Rev. 112, 1303 (1958).

mesons and angle α_p of protons relative to K mesons are plotted as functions of the momentum P. A very desirable feature of the velocity spectrometer as a separation device lies in the fact that very large momentum changes are required in order that pions or protons have the same deflection as K mesons; for example, the spectrometer deflects equally pions with 0.33 Bev/c, K mesons with 1.17 Bev/c, and protons with 2.23 Bev/c. Thus the requirement on the initial momentum selection is mild.

An elementary system utilizing a velocity spectrometer is shown in Fig. 2a. The lens produces at a distance q an image of size I of a target of size 0 located at a distance p. On the way to the lens the beam passes through a momentum analyzer M; on the way from the lens to the image the beam passes through the velocity spectrometer. The crucial quantity is evidently the ratio η of separation S to image size I:

$$\eta = \frac{S}{I} = \frac{\alpha p}{0} \left(1 - \frac{\ell}{2q}\right). \tag{4}$$

The η could be increased by moving the lens to the other side of the spectrometer with a proportional decrease of the acceptance angle $\omega \approx d/p$. Eqqation (4) shows that to utilize the full potentialities of the spectrometer, q should be much larger than ℓ. For this reason the system shown in Fig. 2b was adopted; q is now effectively infinite, hence Eq. (4) becomes

$$\eta = \frac{\alpha p}{0}. \tag{4a}$$

Further impoovement of η can be achieved only at the expense of ω. In fact, since α is inversely proportional to d, it is clear that the product $\eta\omega$ can be improved only by increasing the product $V\ell$ or decreasing the size of 0.[2]

---

[2] For further discussion of optical systems for separators see E. D. Courant and R. Cool, Proceedings of the International Conference on High Energy Accelerators and Instrumentation (CERN, Geneva, 1959), p. 403.

Whether a system such as that proposed in Fig. 2b is, in fact, practical depends on (a) how much bigger the actual images are than those given by geometrical optics, and (b) how well one can prevent scattered pions from sneaking into the K image.

There are many causes that tend to extend the region where particles hit beyond the confines of the geometrical image. Among these, the most important are the chromatic and nonlinear aberrations of the focusing quadrupoles, the multiple scattering of the particles as they pass through the exit thin window of the accelerator, and the "halo" around the target due to decays of pions and strange particles. For all these reasons it seemed desirable to stop the pions in an absorber and use the K-meson image as a source for another complete state of separation. This double separation is shown in Fig. 3.

In comparison with, say, simply doubling the length of the spectrometer, this arrangement offers several distinct advantages. The problem of scattered particles does not exist in the second stage in the same way as in the first stage. Instead, one must be concerned only about the possibility that at the second slit, the image of the first slit, which is out-of-focus due to off-momentum scattered particles passing through it, will overlap the second K-meson image. Such particles can be eliminated by a final bending magnet. The target halo naturally does not exist for the second stage. Finally, the vacuum system required for the spectrometer can be extended through the quadrupole lenses all the way from one slit to the other. Thus multiple scattering is eliminated as a source of undesired particles.

Detailed Consideration of the Apparatus

A sketch of the beam is given in Fig. 4. The secondary particles resulting from the bombardment of a target in the Bevatron are momentum-analyzed by the Bevatron magnetic field. Those with a 1.17-Bev/c momentum move along the indicated trajectory, leave the Bevatron vacuum system through the thin window, and enter the system through a series of collimators placed in a magnetic shield. This shield is located in a large hole cut into the return legs of the Bevatron magnet. The magnetic shield prevents the inhomogeneous magnetic field in this hole from causing aberrations of the target image. The first quadrupole lens system then forms an essentially parallel beam for the spectrometer and the system continues as shown in Fig. 3, except that the fringe field of the final bending magnet is also used for vertical focusing of the beam.

The characteristics of the various components will next be discussed in detail.

Target

The location of the target is established by the requirement that 1.17-Bev/c particles emitted at 0° with respect to the proton beam pass through the center of the hole in the leg slab. The Lawrence Radiation Laboratory has an IBM 650 Code (ETHELBERT) which computes particle trajectories in the median plane of the Bevatron, given the initial position, direction, and momentum of the particles. It can also perform a perturbation calculation to determine their vertical motion once the orbit in the median plane is known. A detailed discussion of the optical considerations of the Bevatron fringe field is out of place here. It suffices to state that at a given momentum the beam is parallel in the horizontal plane and appears to come from a point 79 in. upstream from the upstream end of the first beam-defining collimator in the vertical plane. As a result of aberration studies to follow, the horizontal and vertical apertures of the first quadrupole lens had to be limited to 5.5 in. and 2.0 in., respectively. The corresponding angular apertures at the target were 7.2×10^{-2} radians and 6.0×10^{-3} radians, resulting in an acceptance solid angle of 4.3×10^{-4} sterad.

The height of the target, 0 in Eq. (4) and (4a), is of course of crucial importance for the success of the separation scheme. In the direction of the beam, the thin window had a thickness of 165 mg of Al and hence an rms projected scattering angle of 1.16×10^{-3} radian. At the vertical virtual target position this corresponds to an effective target height of 0.1 in. Since the actual target height is demagnified by a factor of 0.55, a 0.125-in.-high target increases the apparent target height due to multiple scattering by only 15%. Hence a 0.125-in.-high target was adopted.

Tests were run to establish whether a target of this height could be used without loss of beam. In these tests, targets of various shapes made of plastic scintillator were mounted on a pinwheel target holder and viewed directly by a photomultiplier. Compared to a large target, which by hypothesis collected 100% of the beam, targets 0.125 in. high and 0.50 and 0.25 in. along the radial direction collected 70% and 50% of the beam, respectively. A radial dimension of 0.50 in. was selected for the target.

Two targets were chosen such that each could be flipped to the correct position in the Bevatron. One, made of aluminum, was 5 in. in the beam direction, and the other, of tantalum was 3.3 in. long. On the basis of a geometric mean free path for the beam protons and the emitted K mesons, tantalum should give 1.3 times the K yield of aluminum. From a previous associated-production experiment,[3] the K^-/π^- ratio at the target was known to be 0.007 ± 0.003 for 0° and polyethylene; from a previous antiproton experiment,[4] the forward 1.15-Bev/c

[3] Frank S. Crawford, Jr. (Lawrence Radiation Laboratory, private communication.

[4] Cork, Lambertson, Piccioni, and Wenzel, Phys. Rev. 107, 248 (1957).

pion flux from a 6-in.-long beryllium target was known to be in excess of 3700 pions/10^{10} protons/millisteradian/1% $\Delta P/P$. As is shown below, the momentum interval accepted by the system was 2.5%, and the length of the entire apparatus was 1320 in. (so that only 1.9% of the K^- mesons emitted by the target survived). When all these factors, were combined, the minimum expected number of K^- mesons was $0.33/10^{10}$ protons for the aluminum target.

Spectrometers

A cross-sectional view of the velocity spectrometer is shown in Fig. 5. The coils are connected so as to generate a horizontal field; the walls A and B of the iron box serve as pole faces, E and F as return paths. The stainless steel plates C and D provide the coil form and are welded to plates A and B to complete the vacuum enclosure. The electrostatic deflection plates, 230 in. long, were made of 0.063-in.-thick stainless steel sheet 6-3/4 in. wide, and were spotwelded to 2-in.-diameter stainless steel pipe which also went around the ends. As a result of past experience with sparking it was decided to separate the plates 2.5 in. By electrolytic-tank mapping it was found that when the plates were attached 0.125 in. below the tops of the pipes, the field between the plates was constant to 1% to 4 in. from the centerline. A photograph of the plate assembly is shown in Fig. 6.

The uniformity of the electric and magnetic fields is crucial for the success of the separation scheme. At 1.17 Bev/c when the electric and magnetic forces on the K mesons cancel, they fail to cancel for pions by only 7.1%. In order to prevent the spectrometers from introducing significant aberrations, the fields in the region used were held constant to less than 1%. The magnetic field was found to be constant to 0.34%. On the other hand, maintaining the plate spacing constant to 0.025 in. proved troublesome. At the time of installation the mean separations (averaged over the length of the plates) on the two sides of the plates differed by only 0.0006 in. At the end of the bake-out period the difference had increased to 0.009 in. Unfortunately it could not be ascertained what it was at the end of 3 months of operation. Each plate had its own Cockcroft-Walton rectifier--one positive, the other negative with respect to ground. The sum of the two voltages, as metered by a resistive divider, was electronically regulated by controling the input power. The deflected pion beam was used as final voltage standard.

After the spectrometers had been in operation for some time the curve given in Fig. 7, of spark rate of both spectrometers connected in parallel versus voltage was obtained. As a result of this information 380 kv was chosen as the potential between the plates. Towards the end of the run, a 24-hour period, chosen at random, shows a mean spark rate of 0.41 spark per minute, in agreement with Fig. 7. There was therefore no evidence of progressive deterioration (in spite of the fact that a few times air was accidentally admitted to the spectrometers due to forevacuum failures). The spark rate was independent of pressure in the range of 10^{-4} to 10^{-7} mm Hg.

The high-vacuum systems of the spectrometers were extended through the quadrupoles and terminated in 0.020-in. Al windows near the images, as shown in Fig. 4. At the upstream end, where the vacuum system had to be terminated very near the lens for safety reasons, a 0.006-in. Be window was used. A 0.002-in. Mylar bag filled with helium extended from there to the thin window of the Bevatron. The totalm multiple scattering due to the Mylar, helium, and beryllium amounted to 3.5×10^{-4} radian and increased the effective height of the virtual object to 0.148 in.

From Eq. (2) and the data of this section, α_{π} at 1.17 Bev/c is 2.32×10^{-3} radian. The magnetic field required in order that the K mesons satisfy Eq. (1) is 216 gauss.

Beam Optics

Substituting the appropriate quantities into Eq. (4) gives $\eta = 2.88$ if the target is taken to be 0.148 in. high and uniformly illuminated (rather than the actual multiple-scattering Gaussian distribution). This does not leave much margin for poor focusing and aberrations. Therefore, the quadrupoles and the bending magnet were subjected to a careful study.

For these studies the usual wire-orbit method was used, but considerable effort was devoted to increasing its precision. Wherever the position of the wire had to be measured in space low power microscopes were mounted on a rectangular frame which could be moved in the plane perpendicular to the wire by means of lead screws. Wire-position measurements were then generally reproducible to 0.3 mm. Both because the optics of the beam required it and because it facilitated the treatment of the quadrupole as a thick lens in subsequent calculations, the wire was always sent into the focusing device parallel to the optic axis. As a result, focal points and principal planes could be established at once.

Each quadrupole lens consisted of three 8-in.-bore sections, the outside ones 16 in. long and the central one 32 in. The sections were spaced 9 in. apart. In order to avoid an excessive number of free parameters and also to have principal planes located symmetrically about the quadrupole, the two outside sections were operated at the same current. Figures 8 and 9 show examples of the chromatic and nonlinear aberrations for such a lens system when it was adjusted so that the CDC (convergent, divergent, convergent) and DCD focal points coincided 152 in. from the center of the lens system. The nonlinear aberration curve is that for the aberration which is of greatest interest for the beam geometry of this experiment: the variation of the focal length in the vertical plane for paraxial rays as they are displaced horizontally. As a result of such measurements the DCD condition was selected for the more critical vertical plane in spite of its greater chromatic aberration. The character of the nonlinear aberration suggests that it is primarily due to imperfections of the field configuration.

Preliminary measurements of the same aberration on the final bending magnet (36 in. long, 18 in. wide, with a 4 in. gap, and required to produce to 30° bend) showed that its focal length in the vertical plane varied by more than a factor of two when the rays were displaced laterally by 4 in. This was due in part to the fact that the constant field lines were not parallel to the iron edges and in part to nonuniformities of the field inside (at 19,500 gauss). It was found that this condition could be corrected by increasing the gap to 8 in. and placing shims along the side edges of the pole faces as shown in Fig. 10a; the field at the center of the magnet then varied from one side to the other as shown in Fig. 10b, and the focal point in the vertical plane varied as shown in Fig. 10c. The abscissa in this case is the horizontal position where the wire crossed the center of the magnet. Evidently there now exists an 8-in.-wide region where the focal length varies by less than $\pm$ 7.5%.

A sketch of the optical arrangement finally chosen is shown in Fig. 11. With regard to the horizontal plane, it should be observed that the first quadrupole forms a real image of the target in the second quadrupole, and the final quadrupole forms an image of this image at the second slit. Because of the momentum dispersion due to the Bevatron field, images of different momenta, then appear along the H line in the second quadrupole. A collimator situated in this region was used to define the momentum interval transmitted to the remainder of the apparatus.

As a result of vertical-image-profile calculations based on the measurements of chromatic and nonlinear aberrations, this collimator was chosen to transmit a 2.5% momentum interval. In the horizontal plane, the second quadrupole thus served as a field lens directing off-momentum particles back into the third quadrupole. At the second slit the horizontal image of the 0.5-in.-wide target was 3.7 in. The momentum dispersion at the second slit was 3.34 in./1% $\Delta P/P$, of which 1.02 in./1% $\Delta P/P$ due to the final bending magnet.

It will be observed that in the vertical plane the beam is slightly convergent within the velocity spectrometers. In the second half of the system this was dictated simply by the focal length of the shimmed bending magnet, but in the first leg the convergence was introduced deliberately so that off-momentum particles would not strike the spectrometer deflection plates. The vertical magnification of the first system was 0.88, that of the second, 1.68; the expected separation between the pion and K^- meson images was 0.336 in. for the first system, and 0.464 in. for the second.

Backgrounds

Thus far the discussion has dealt primarily with what one might call the "rational" beam. In addition one expects the presence of an "irrational" beam due to pions scattered from various surfaces, emitted from sources other than the target, and muons resulting from $\pi \rightarrow \mu$ decay in flight. Because of the large number of particles that enter the channel and are available for scattering, estimates of the intensity of the "irrational" beam reaching the chamber are bound to be unreliable. Much effort was devoted to minimizing the "irrational" beam. However, as no serious calculations were made and during the experiment no time could be allotted to the determination of the efficiency of various collimation arrangements, it is quite possible that some of the precautions were unnecessary. A drawing showing the location of all the collimators is given in Fig. 12.

The following "philosophy" was used as a guide in the design of the collimation system. It was assumed that the first separation system could not be made very effective because of multiple scattering in the thin window, target halo, and scattering from beam-defining collimators--all unavoidable in the first stage. In the second stage, on the other hand, these effects are not present. It seemed possible therefore to make the second stage essentially perfect. The aim was then to arrange the second stage in such a way that a pion or muon coming through the first slit could not pass through the second, <u>no matter what its momentum</u>, barring $\pi \rightarrow \mu$ decay or scattering from the vacuum chamber walls near the final bending magnet. The method for doing this is illustrated in Fig. 13. Let K and π be the K-meson and pion images at the proper beam momentum and let π' be the image of pions of some lower momentum P'. The dotted lines are the extreme trajectories of particles passing through the π' image. Clearly the lower trajectory just begins to pass through the K image. Hence scattered pions can get through the K slit only if their momentum deviation is $\Delta P \geq |P' - P|$. Now, if the dispersing action of the bending magnet is such that particles with $\Delta P \geq |P' - P|$ are deflected beyond the lateral limits of the K slit, none can get through at all. This is suggested by Fig. 13b. The purpose of the vertical collimator in the third quadrupole was to limit δ (Fig. 13a) for scattered particles.

Although the second stage can be made opaque to pions and muons, at least in principle, there still remains the possibility that a pion coming through the first slit decays before reaching the second and the decay muon passes through the second slit. For a 0.32-in.-high second slit the probability of this is 0.6% to 0.9% per pion admitted through the first. It is therefore important to keep the number of pions transmitted through the first system small even if the second system is perfect. The same requirement applies in order that pion scattering in the second stage be negligible compared with the "rational" beam.

A rough calculation shows that, when pions hit 0.15 in. from the jaws of a uranium slit, $\sim$15% enter the slit through the side because of multiple scattering (for muons this fraction is considerably greater, since they do not suffer nuclear attenuation). Of the pions entering the first slit in this fashion, only $\sim$1% are within the solid angle accepted by the second separation stage. For particles entering the second slit through its side the probability of passing into the bubble chamber is $\sim$5%. Although these numbers are small, it seemed desirable to suppress such particles more efficiently. For this reason the slits and also some of the critical collimators were made of Armco iron and magnetized so that negative particles passing through the iron would be deflected out of the beam. To reduce the power requirements and to avoid stray fields, side pieces were added in such a way that each slit formed a closed magnetic circuit. In Fig. 12 the dotted lines behind the slits and the iron collimators indicate the deflection of particles that have passed through the entire length of magnetic field. Uranium blocks were placed behind each of these magnetized devices to stop the deflected particles.

In the vertical plane the collimation system of the first stage consists of only one magnetized iron collimator placed at the entrance to the first quadrupole and backed up by a uranium catcher at the center of the lens. The collimator faces were sloped to aim at the edges of the virtual target.

In the horizontal plane particles far removed from the beam momentum are eliminated by two iron collimators placed ahead of the first quadrupole. Since particles passing through the first iron collimator at a large angle could be deflected into the general beam direction by the magnetic field in the collimator iron, a uranium collimator was placed ahead of it to cover the critical region. A large amount of scattering due to off-momentum particles was expected from this collimator system. Therefore another collimator was placed ahead of the third quadrupole, at the point where the second quadrupole forms an image of the front collimators. It was expected that a large fraction of these scattered particles, especially those in the critical momentum region near the beam momentum, could be removed in this fashion.

Finally, those particles whose momenta were close to the beam momentum were stopped in the momentum-defining collimator in the second quadrupole. In this connection it should be mentioned that the spectrometer is a very efficient collimator itself. If a particle has a momentum such that it leaves the spectrometer plates from the side then, upon leaving, it experiences the magnetic force without the bucking electric force. Hence it is deflected sharply out of the median plane before it hits the vacuum-chamber wall. The mild convergence of the beam between the plates was chosen so that pions would leave the plates on the sides before they collided with the upper plate regardless of their momentum.

The pions were deflected upward in the first spectrometer so that the pion image of the target holder would not overlap the K image. In the second stage the pions were deflected down. This was based on the idea that those pions and muons which managed to get through the first slit iron would appear to enter the second stage from a source located somewhat above the first slit and would be imaged somewhat lower at the second slit.

Beam Tests

After the apparatus had been assembled and aligned by means of optical levels, and the vacuum systems had been put into operation, the lenses were refocused, using pions. The profile at the first slit position is shown in Fig. 14, the counter size and the position of the expected K image are also indicated. When the counter size is unfolded from this profile a full width of 0.166 in. at half maximum is found. This image size should be compared with a full width of ~0.15 in. obtained by folding the demagnified image of the multiple-scattering virtual source of 0.148 in. with the aberrations of the first stage. The second stage was designed to be opaque to pions for a 0.1-in.-high slit. However, this would have caused a 35% loss of K mesons; since a high K-meson yield seemed more important than complete pion suppression, a 0.200-in.-high first slit was chosen. The nature of the particles far out in the wings of the distribution was investigated by an absorption experiment, which showed them to be pions and muons in a ratio of roughly 3:1. At the position of the K slit, the flux is ~3% of the value found at the pion peak and presumably consists mostly of pions.

The image at the second slit had a full width at the half maximum of ~0.32 in. as expected for a 0.2-in. source and a magnification of 1.68. Accordingly, a 0.326-in.-high second slit was selected.

Next, the deflection sensitivities of the spectrometers were determined by observing the motion of the image out of the median plane when small currents were sent through the spectrometer coils with no potential applied to the plates. These were found to be 45 amp/in. and 32.5 amp/in. for the first and second stage, respectively; these numbers are in agreement with the spectrometer excitation coefficient of 240 gauss in./amp and the focal lengths of the second quadrupole and the bending magnet.

When the system is working properly the K mesons go through undeflected and the pions experience a small magnetic force. This force can be "mocked up" without the need for an electric field by putting appropriate small currents into the spectrometers. The relative particle flux obtained by counting behind the second slit as the two spectrometer currents were increased together is shown in Fig. 15. The dotted line was obtained by subtracting the counting rate obtained with a 12-in. Pb absorber between the counters and is thus primarily due to pions. Also shown in the figure are the potential between the plates corresponding to each current setting and the expected relative K flux at the second slit. Thus according to these measurements a 33% pion back ground and a 67% muon background were expected at 380 kv. The second stage therefore suppressed pions by a factor of 1000. The curve also shows that if the currents are increased by a small amount ΔI beyond the point at which K mesons satisfy Eq. (1), a considerable suppression of pions can be achieved at the expense of a slight loss of K mesons. For example, if both currents are increased by 1.50 amp, 30% of the K mesons are lost but the pion background is then only 11%.

In order to steer the K mesons through the two slits the following method was employed. Sandwiches of three 0.19-in. -high scintillators were mounted so that each was viewed by an individual 1P21 photomultiplier. One such "triad" was mounted on ways in front of each slit such that it could be displaced above or below the slit by an easily measurable amount. The output currents of the photo-multiplier charged capacitors whose potentials were displayed in succession on an oscillograph by means of a relay-actuated sampling device. A photograph of a typical oscillograph trace is shown in Fig. 15. (The displaying time of one of the capacitors was lengthened deliberately in order to avoid confusion between the two triads.) Now, in order to steer K mesons through the slits, the center "triad" counters were first placed in front of the slits, and the spectrometer currents required to steer pions through the system were noted. The spectrometer currents were then increased by a factor of 1.0765, corresponding to the ratio of pion and K-meson velocities. At the same time the triads were displaced according to the known deflection sensitivites in such a way that the pions again struck the center triad counters. The apparatus was then tuned for K mesons and the triads served as a pulse-by-pulse monitor of proper steering. The system essentially amounts to using the pions as an electrostatic voltmeter.

It remains to discuss the results of measurements of the beam properties using the bubble chamber itself. The total K flux through the chamber was readily obtained by counting K decays and dividing by the well-known decay probability within the chamber (4.15%). Averaged over all kinds of operating conditions, the K flux during the experiment was $0.87/10^{10}$ protons. This flux is roughly three times that expected. Since this greater yield is not accompanied by a better pion rejection than that predicted on the basis of Fig. 15, it appears likely that the pion-flux estimate used was too conservative. The K-meson yield from the Ta target was ~20% higher than that from the Al target. The pion contaminations from the two target materials were the same within errors.

The cross section for the production of δ rays with energy $E_\delta \geqslant 5.83$ Mev by a pion of ~1.1 Bev/c is 28 mb, while that for K mesons is zero. Hence, when a track is observed which has a δ ray with $E_\delta \geqslant 5.83$ and then has a nuclear interaction, the track can be identified as being due to a pion. Then, by use of the approximate cross section of 43 mb for the production of visible two-pronged pion events given by Baggett,[5] the total number of pions may be deduced. The pion contaminations are given in Table I for two operating conditions, (a) when both spectrometers were tuned to the K-meson peak and (b) when the current in the second spectrometer was increased, first by 3 amp and later by 2 amp beyond the K peak.

In addition to K mesons and pions, the beam contained a large number of muons, some satisfying all beam criteria, some of considerably lower momentum, etc. For the two operating conditions the analysis of all tracks in two typical rolls of film (about 350 pictures per roll) leads to the breakdowns given in Table II.

Table I

Pion contaminations

Spectrometer settings	π/K Ratio
$\Delta I_1 = 0$ $\Delta I_2 = 0$	50 ± 18%
$\Delta I_1 = 0$ $\Delta I_2 = 2$ to 3 amp	8 ± 11%

Table II

Track analysis for two typical film rolls

Spectrometer settings	Protons on target	Analysis				
		All tracks	Beam tracks	Beam K mesons	Beam pions	Beam muons
$\Delta I_1 = \Delta I_2 = 0$	6.8×10^{12}	3722	1467	534	202	731
$\Delta I_1 = 0$, $\Delta I_2 = 2$ to 3 amp	7.8×10^{12}	3597	1256	596	35	625

[5] Lee Baggett, Jr., π^--p Elastic Scattering in Single-Pion Production at 0.939 Bev/c (thesis), UCRL-8302, May 28, 1958, unpublished.

For the design of future beams it is of considerable interest to understand how the pions found in the chamber managed to get there. The following remarks summarize the properties of the pion component:

(a) The pions are in a momentum band ranging from 1.12 Bev/c to 0.75 Bev/c with a relatively sharp upper edge.

(b) Pions of all momenta are uniformly distributed in horizontal position in the chamber.

(c) Pions tend to enter the chamber 1.5 cm higher than the K mesons.

An examination of Fig. 14 shows that some pions from the wings of the pion image are admitted to the second stage when the system is tuned to K mesons. Owing to chromatic aberrations in the first stage these pions are likely to have deviations of about 2% from the central momentum. Furthermore, the nonlinear and chromatic aberrations in the second quadrupole tend to cancel for high momenta, but add for low momenta; hence the momentum in the wings of the pion image is likely to be 2% low. According to the discussion accompanying Fig. 13 such particles cannot come through the second slit. But that discussion did not include the nonlinear aberrations in the second system; if these are included such particles can just barely get through. This explains the sharp upper momentum edge of the pions. The lower-momentum pions are then those which passed through varying amounts of the second-slit iron. They arrive high in the chamber because that is the only direction in which they can escape the magnetic field in the collimator. If this is the correct explanation for the pion component then the decision to deflect the pions downward in the second stage might have been an incorrect one. An examination of the vertical-plane optics shows that (neglecting the slight convergence of the beam in the spectrometers and differences in focal lengths) if, because of aberrations, an off-momentum particle manages to get from the target to the first slit after being deflected upward in the first spectrometer, then, by symmetry, it will also pass through the second slit provided the spectrometer is arranged to deflect it down.

After the end of K^- experiment the beam was tuned up for antiprotons. At 380 kv the pions would have been deflected into the spectrometer plates, which would have made the triads useless and possibly would have increased the scattered-particle flux. For this reason the potential between the plates was reduced to 200 kv. The antiproton yield was then found to be $0.5\ \bar{p}\ /10^{11}$ protons, and the $\bar{p}:\pi:\mu$ ratio with rather mild beam criteria was 33:7:60.[6]

[6] Sulamuth Goldhaber, Lawrence Radiation Laboratory, private communication.

Acknowledgments

It would be difficult to acknowledge the advice and assistance of all those whose aid was required during the design and construction of this beam. First of all, we wish to thank Professor Luis W. Alvarez for his encouragement and support. Mr. Bruce B. Cork and Dr. William A. Wenzel contributed invaluable advice concerning the construction and operation of the spectrometers. Mr. Glen R. Lambertson advised us on the difficult magnetic shielding problem in the leg slab area.

The invaluable cooperation of Dr. Edward J. Lofgren and the Bevatron crews is gratefully acknowledged. We wish to thank Messrs Lazarus G. Ratner and Joseph H. Dorst for their help during the extended wire-orbit and magnetic-field measurements. Mr. William W. Salsig and the Lawrence Radiation Laboratory engineering staff relieved us of all worries regarding mechanical design. In particular, Mr. George W. Edwards designed the complex vacuum extensions of the spectrometers.

The operation of the hydrogen bubble chamber was under the direction of Mr. James Donald Gow. The chamber crews, with Messrs Robert D. Watt and Glenn J. Eckman acting as crew chiefs, not only did a splendid job operating the chamber but also provided invaluable help with the high-voltage and vacuum systems of the spectrometers.

Last, but by no means least, we wish to acknowledge the assistance of Messrs. William Graziano and Stanley G. Wojcicki. Without their tireless and consciencious help the project could not have succeeded.

Legends

Fig. 1. Angle of deflection a_π of pions relative to K mesons, and a_P of protons relative to K mesons versus momentum, $P_0 = V\ell/d$, where V is the potential across the plates in Mv and ℓ and d are the plate length and separation, respectively.

Fig. 2. Simple optical arrangements for use in connection with a velocity spectrometer.

Fig. 3. Schematic arrangement for double separation system.

Fig. 4. Complete layout of 1.17-Bev/c K^- beam.

Fig. 5. Cross section through spectrometer.

Fig. 6. Photograph of spectrometer plate assembly.

Fig. 7. Spark-rate curve for <u>two</u> spectrometers.

Fig. 8. Chromatic aberrations of 8-in. quadrupole lens triplet.

Fig. 9. Nonlinear aberrations of 8-in. quadrupole lens triplet.

Fig. 10. Nonlinear aberration of shimmed bending magnet.

Fig. 11. Schematic optics of 1.17-Bev/c beam.

Fig. 12. Arrangement of collimators for 1.17-Bev/c K^- beam.

Fig. 13. Sketch to illustrate scheme for making second separation stage opaque to all pions.

Fig. 14. Measured beam profile at the first slit position.

Fig. 15. Measured pion attenuation of the entire apparatus.

Fig. 16. Triad display pattern.

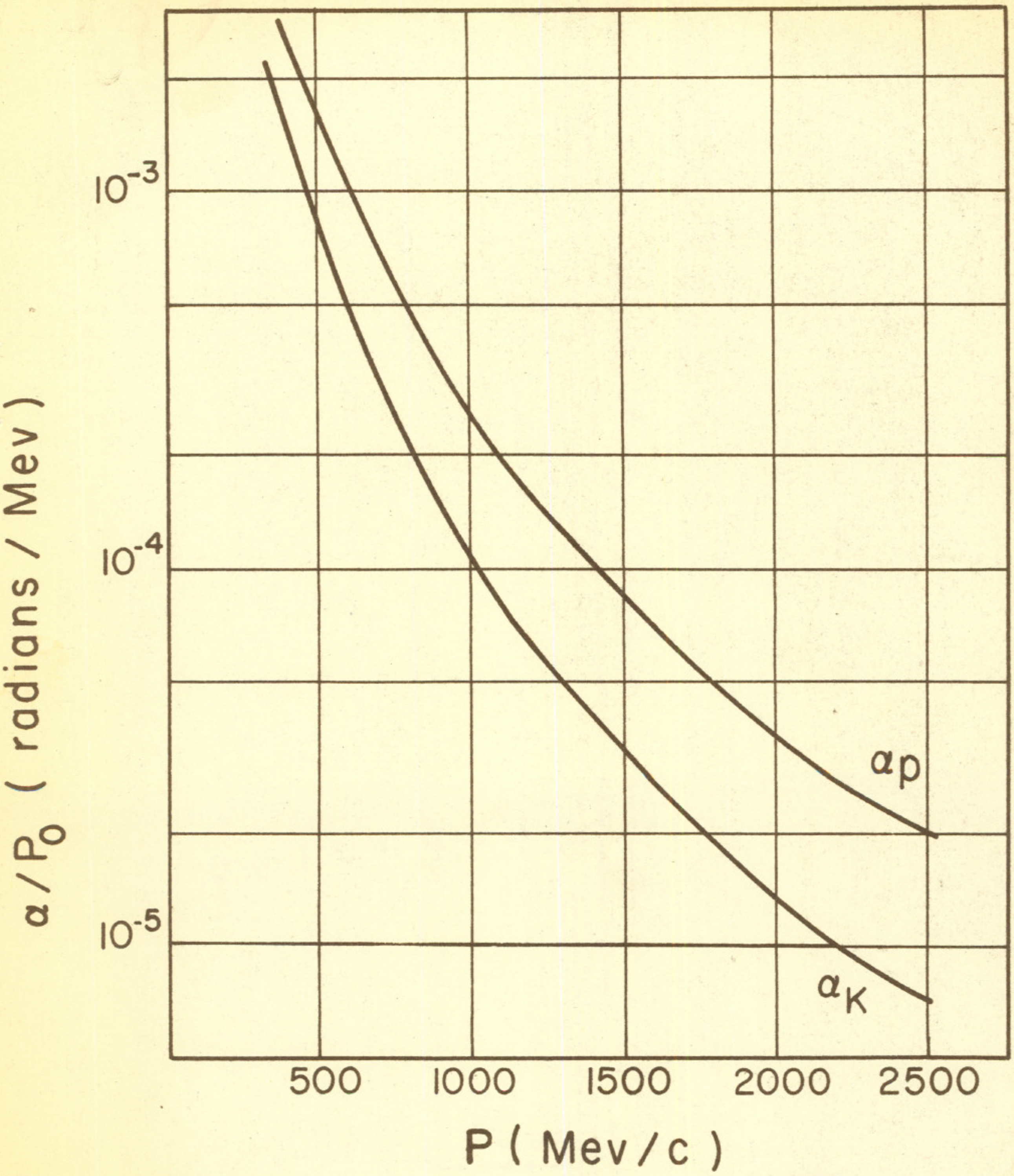

Fig 1

61

55,886-1

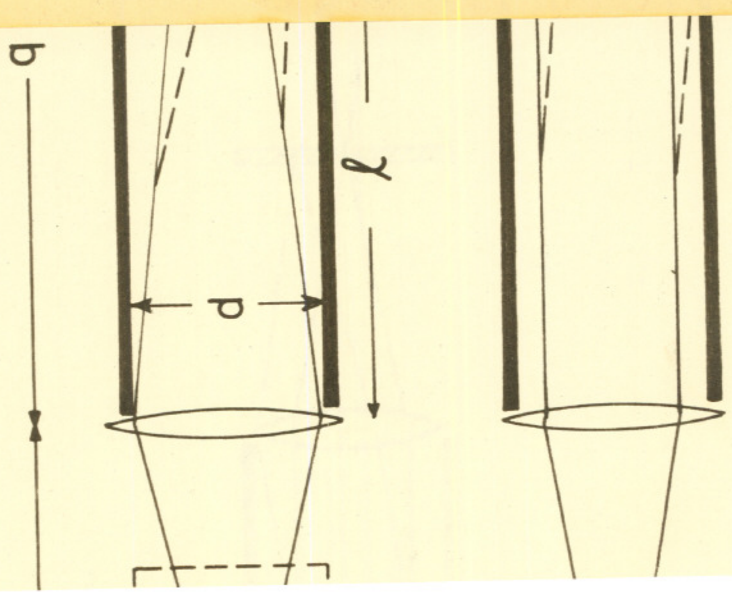

Fig 2

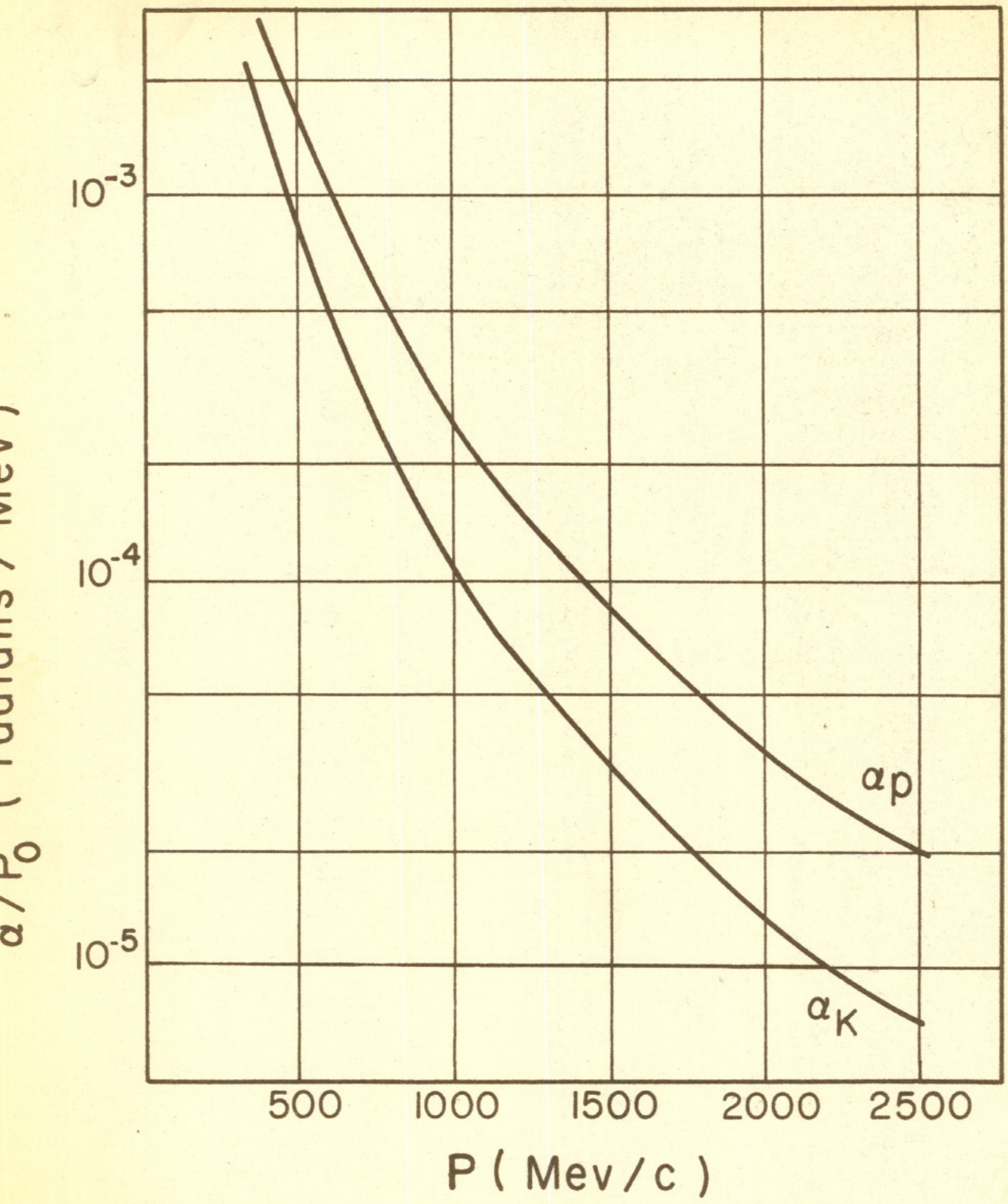

Fig 1

61

1-98855

55,886-1

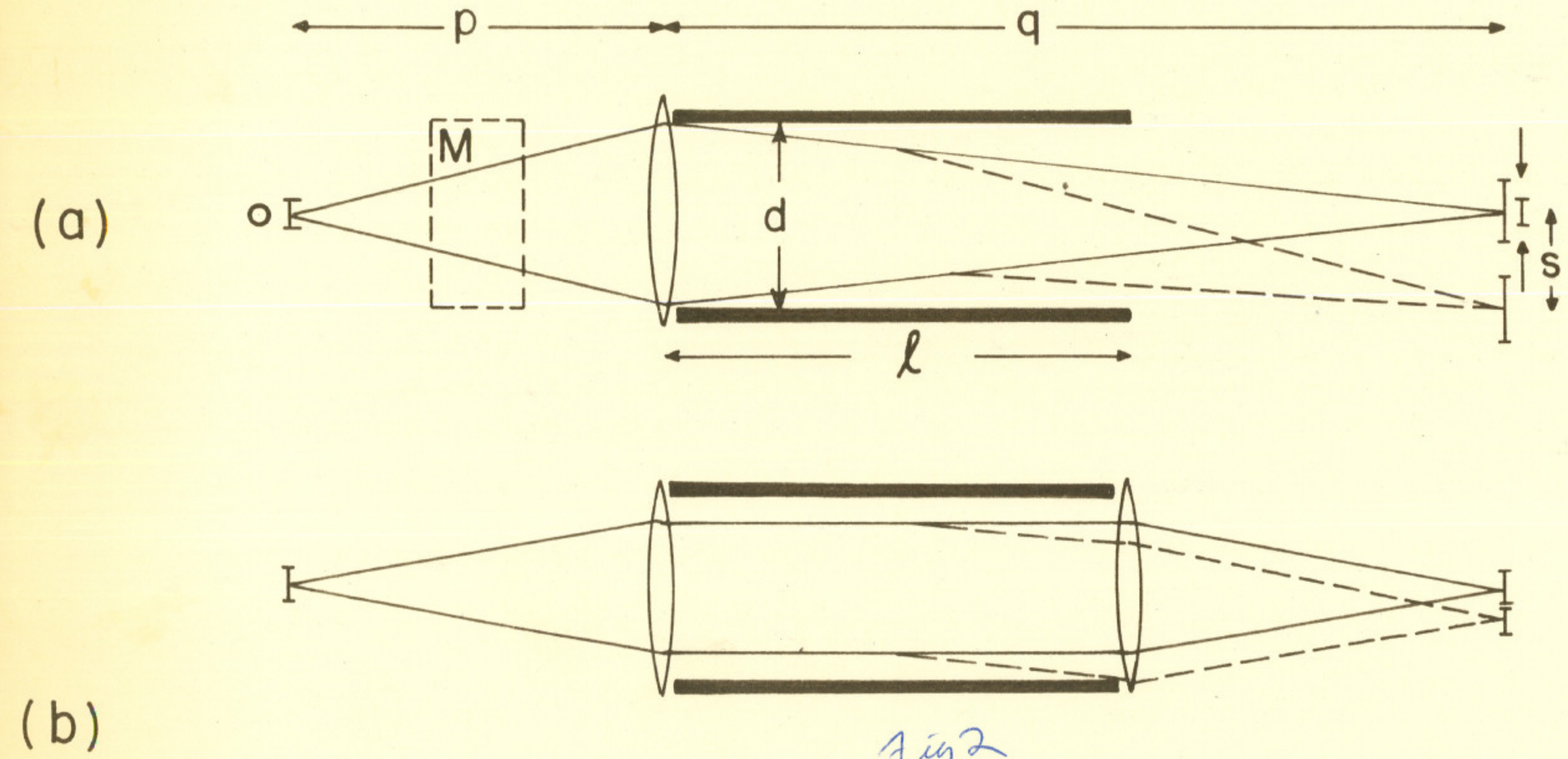

Fig 2

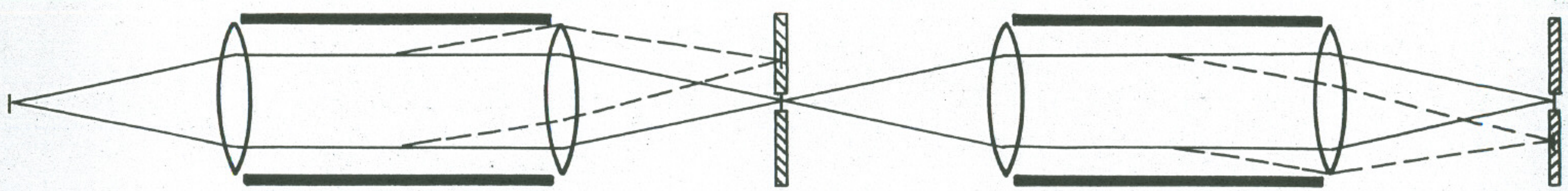

Fig3

59

55,912-1

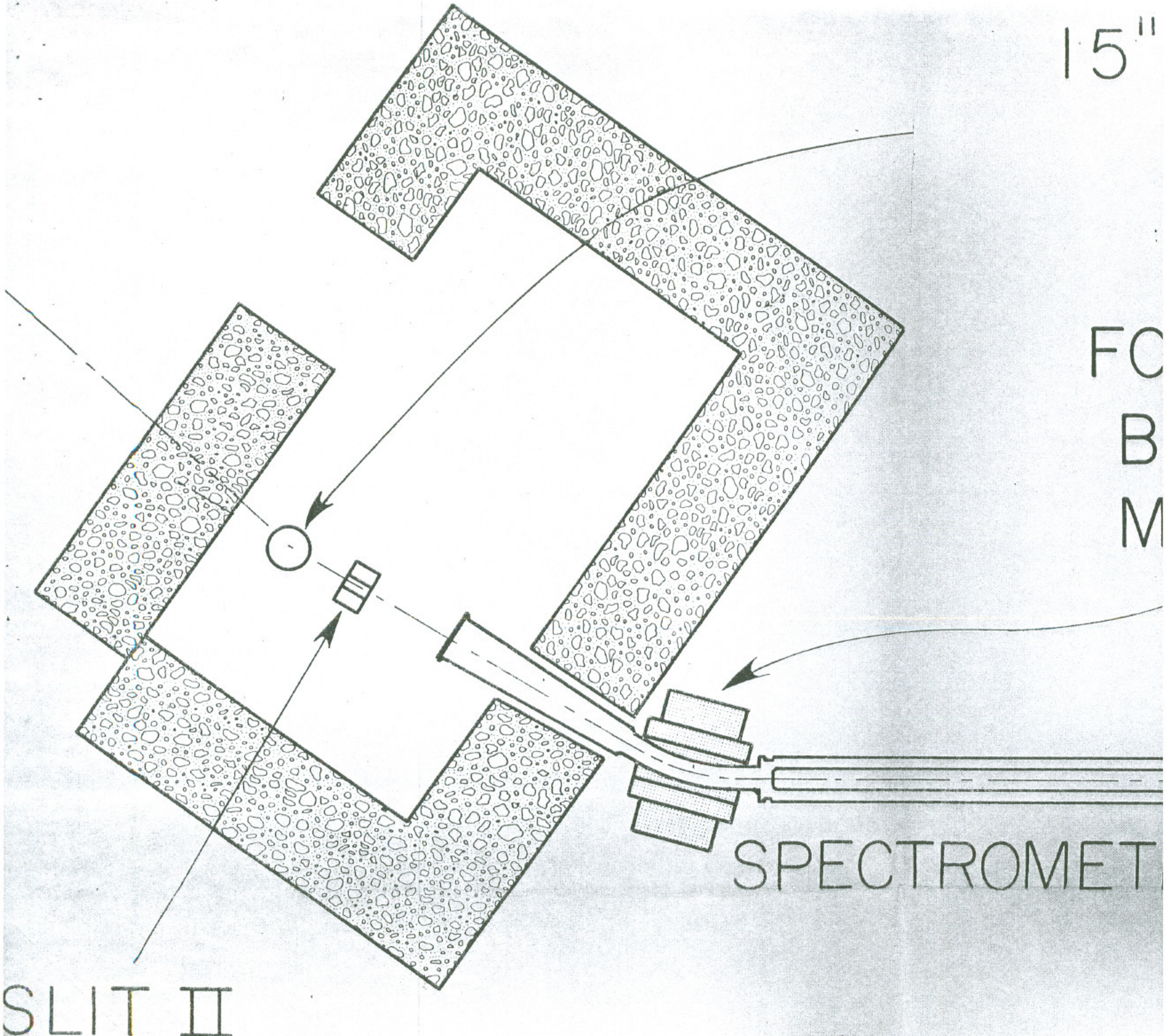

Fis. 4A

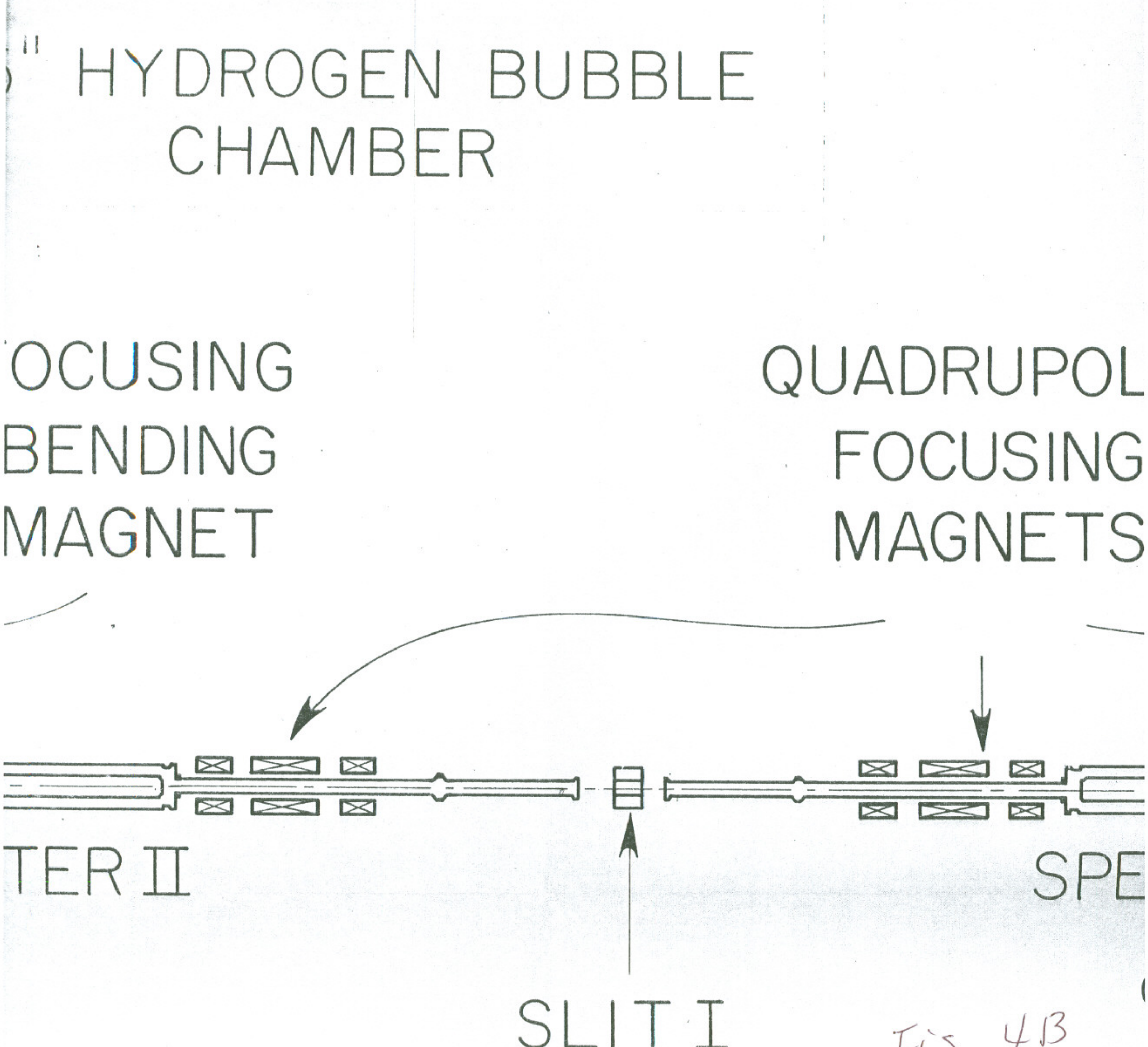

" HYDROGEN BUBBLE
CHAMBER
OCUSING
BENDING
MAGNET
QUADRUPOL
FOCUSING
MAGNETS
TER II
SPE
SLIT I

Fig. 4B

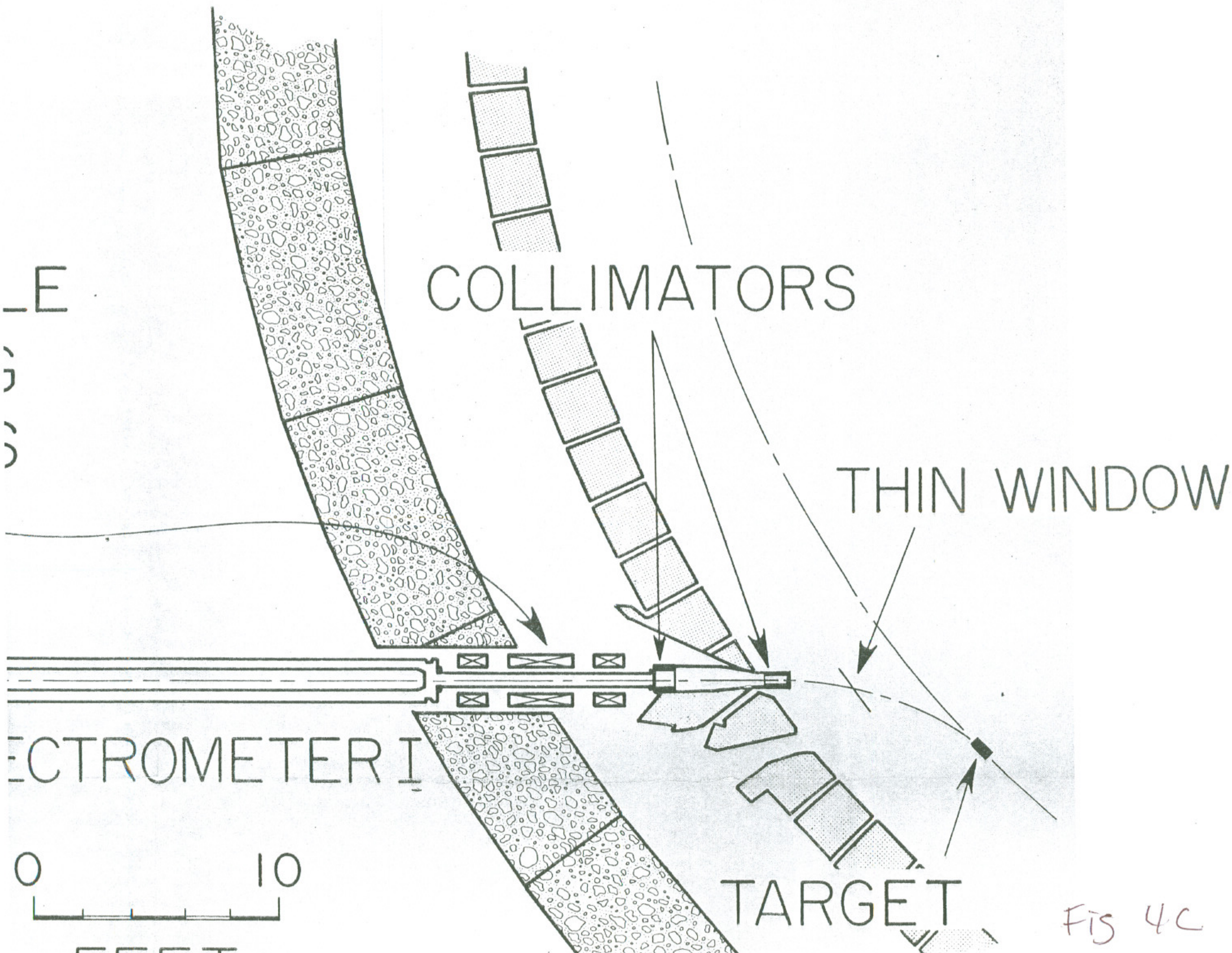

Fig 4C

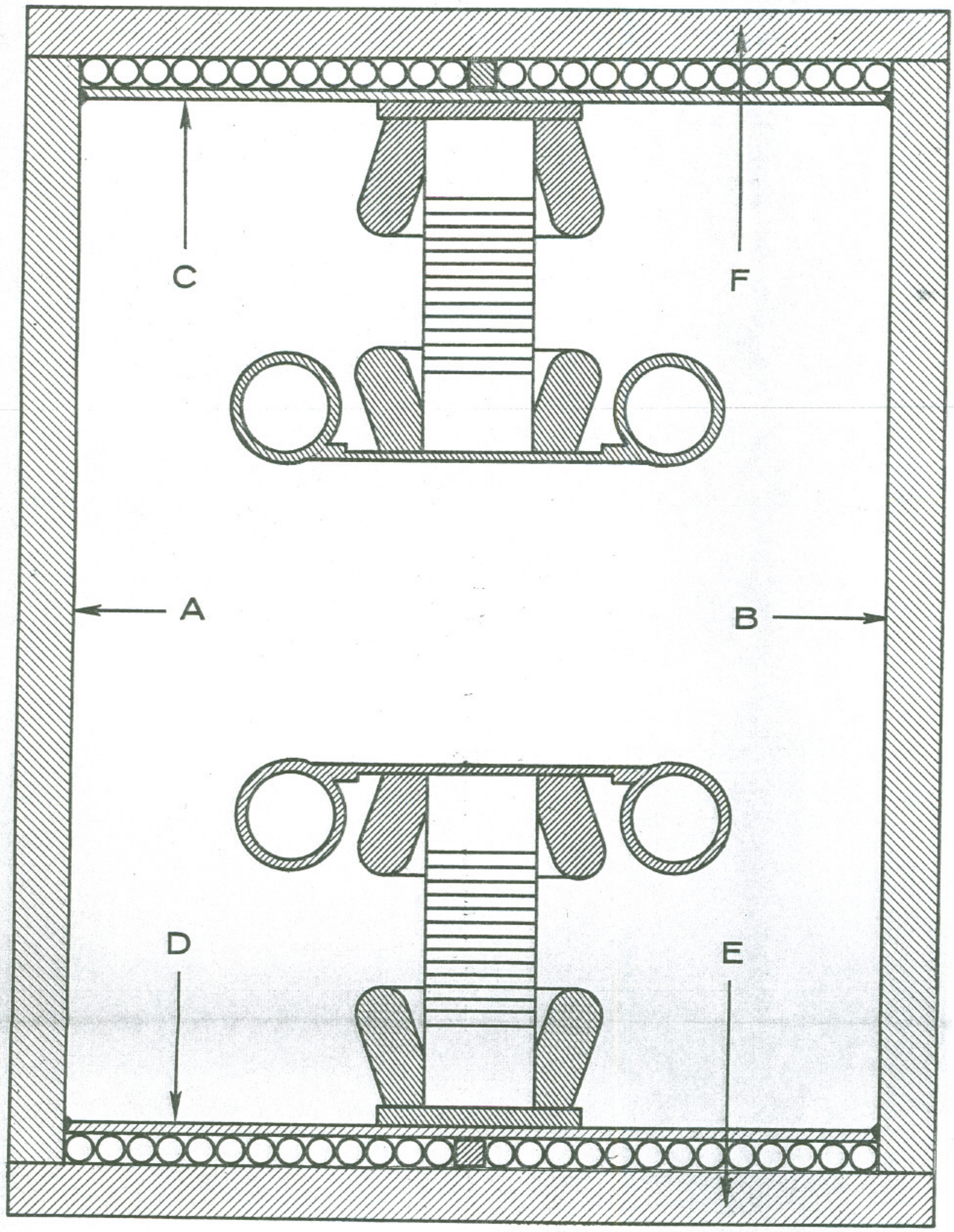

Fig. 5

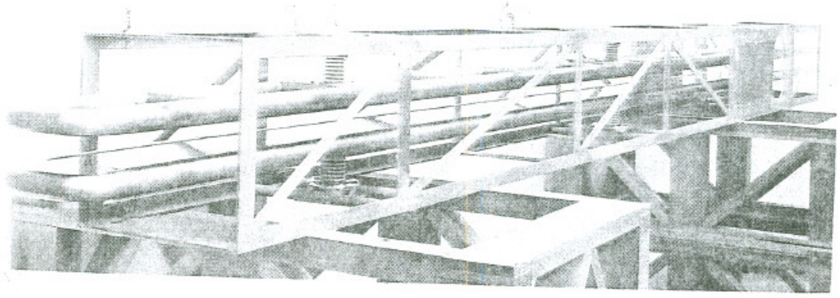

Fig. 6

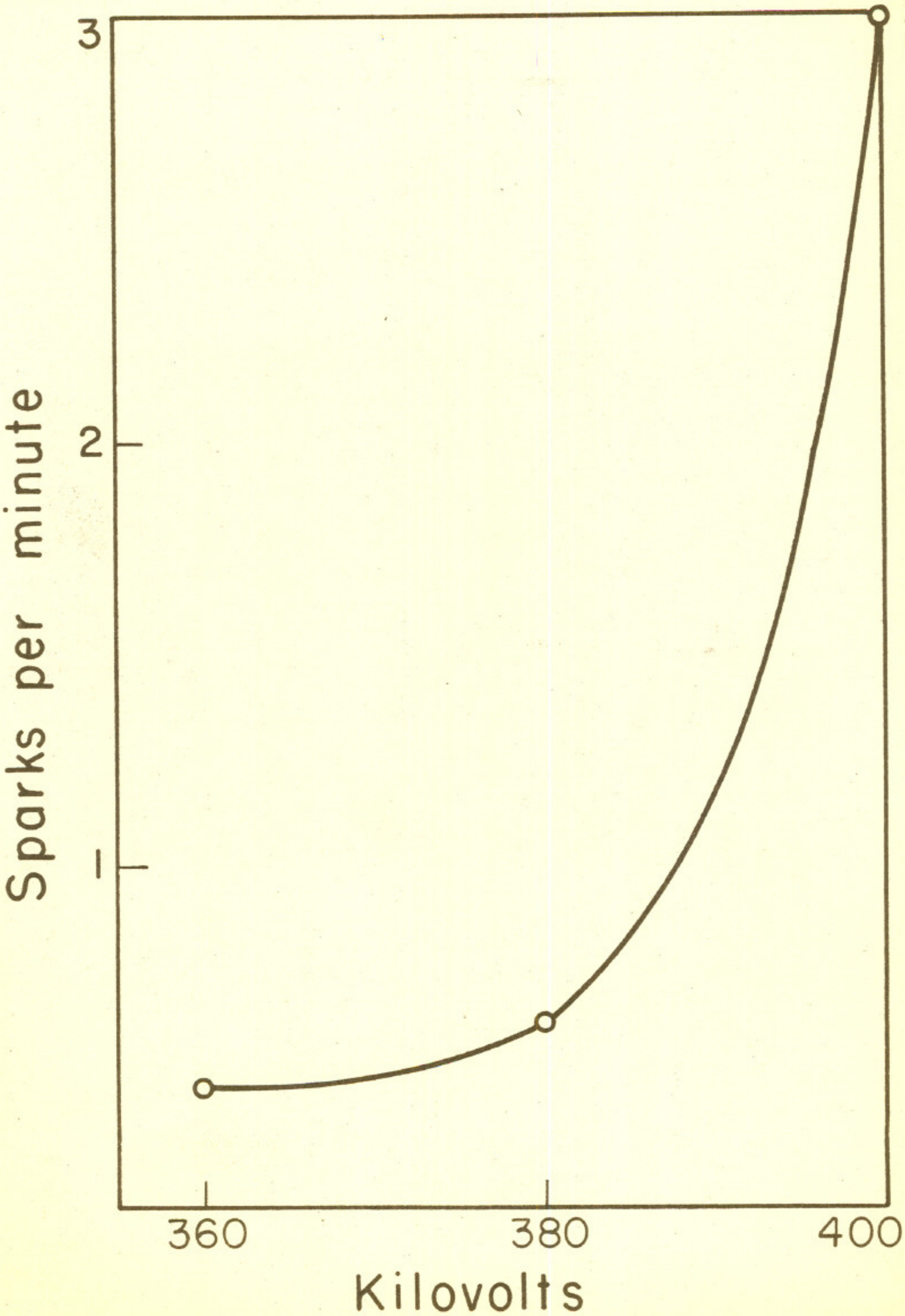

Fig 7

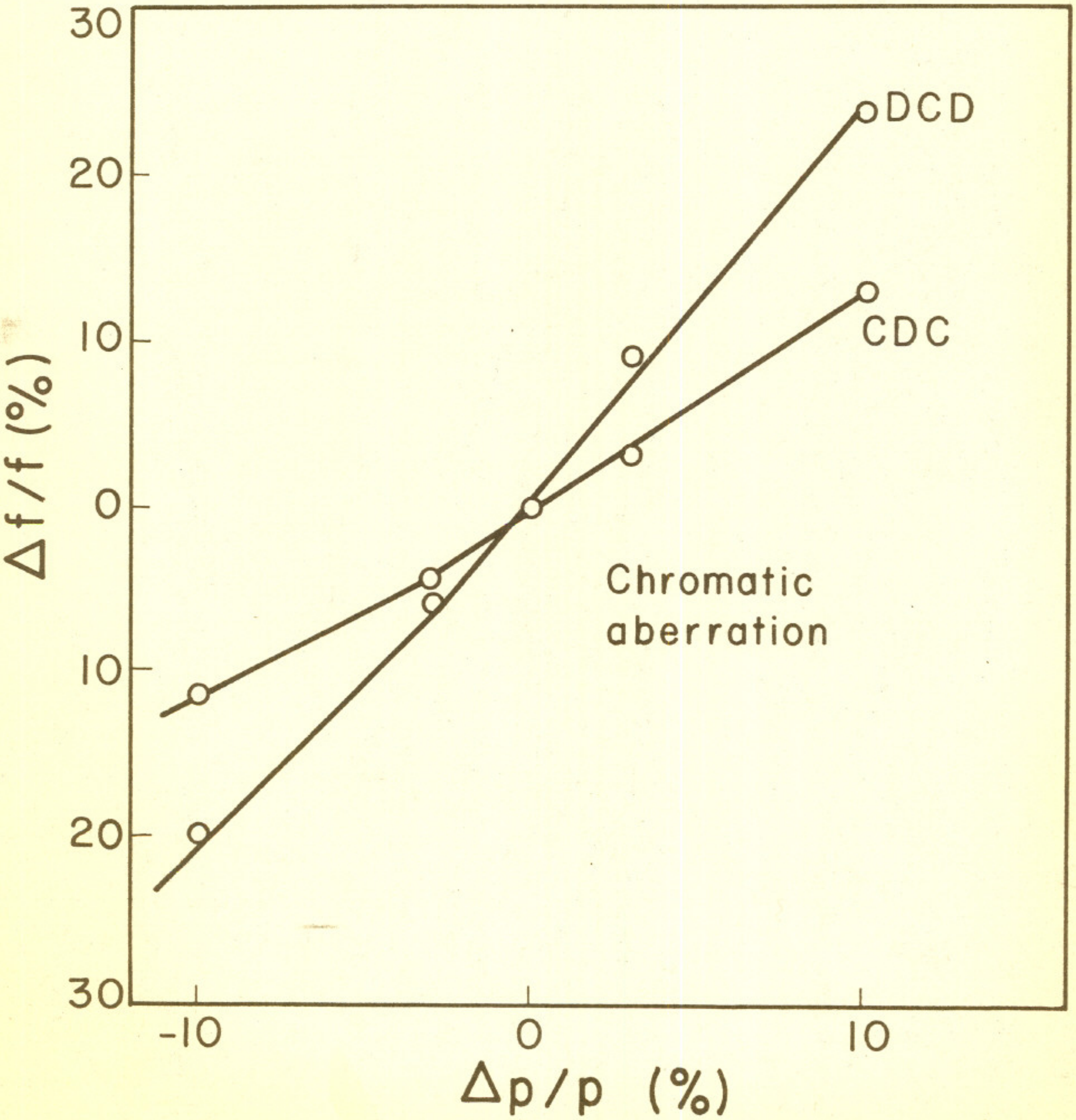

Fig 8

65

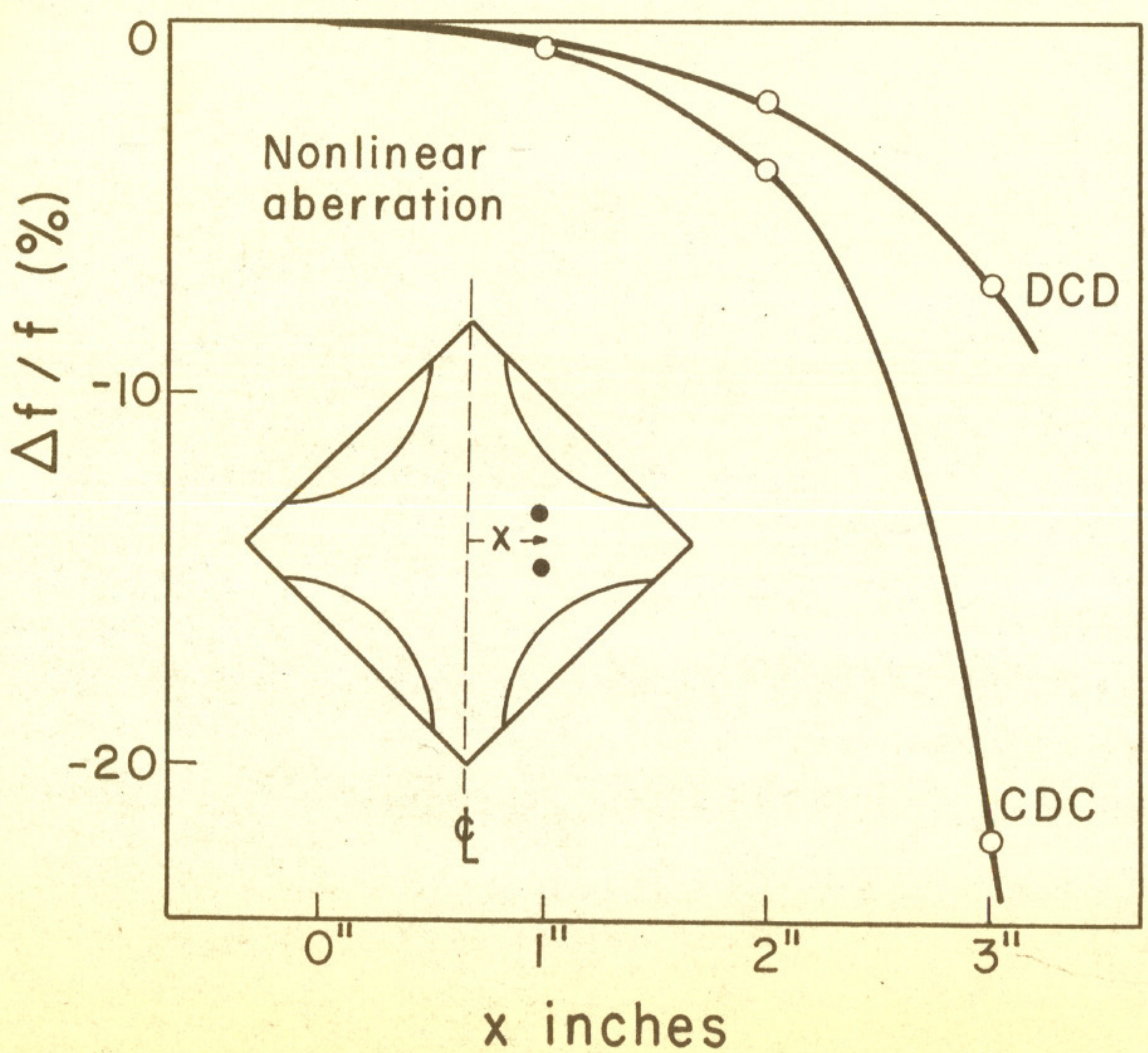

Fig 9

55,925-1

0010030390 0

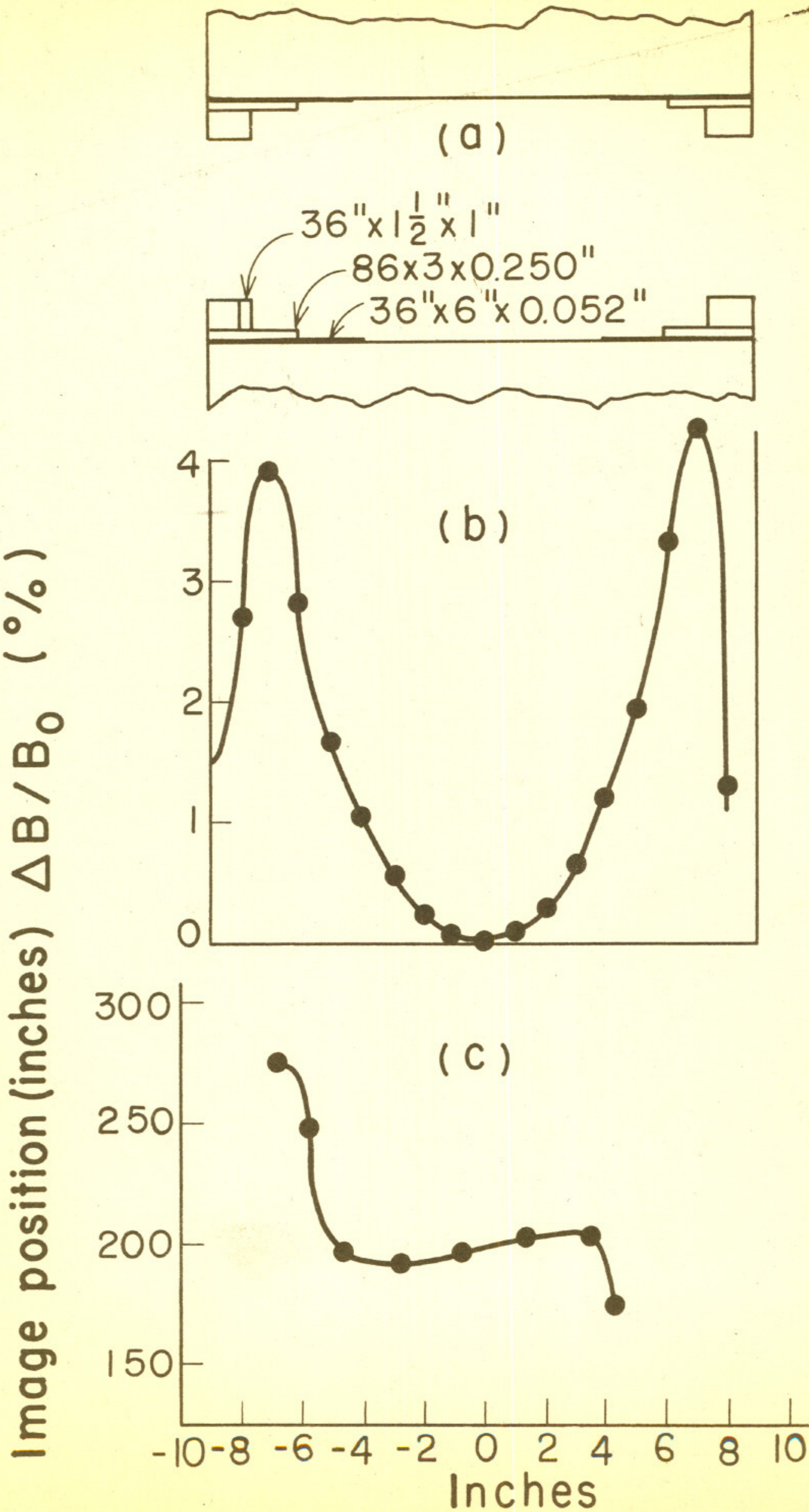

Fig 10

55,886-1

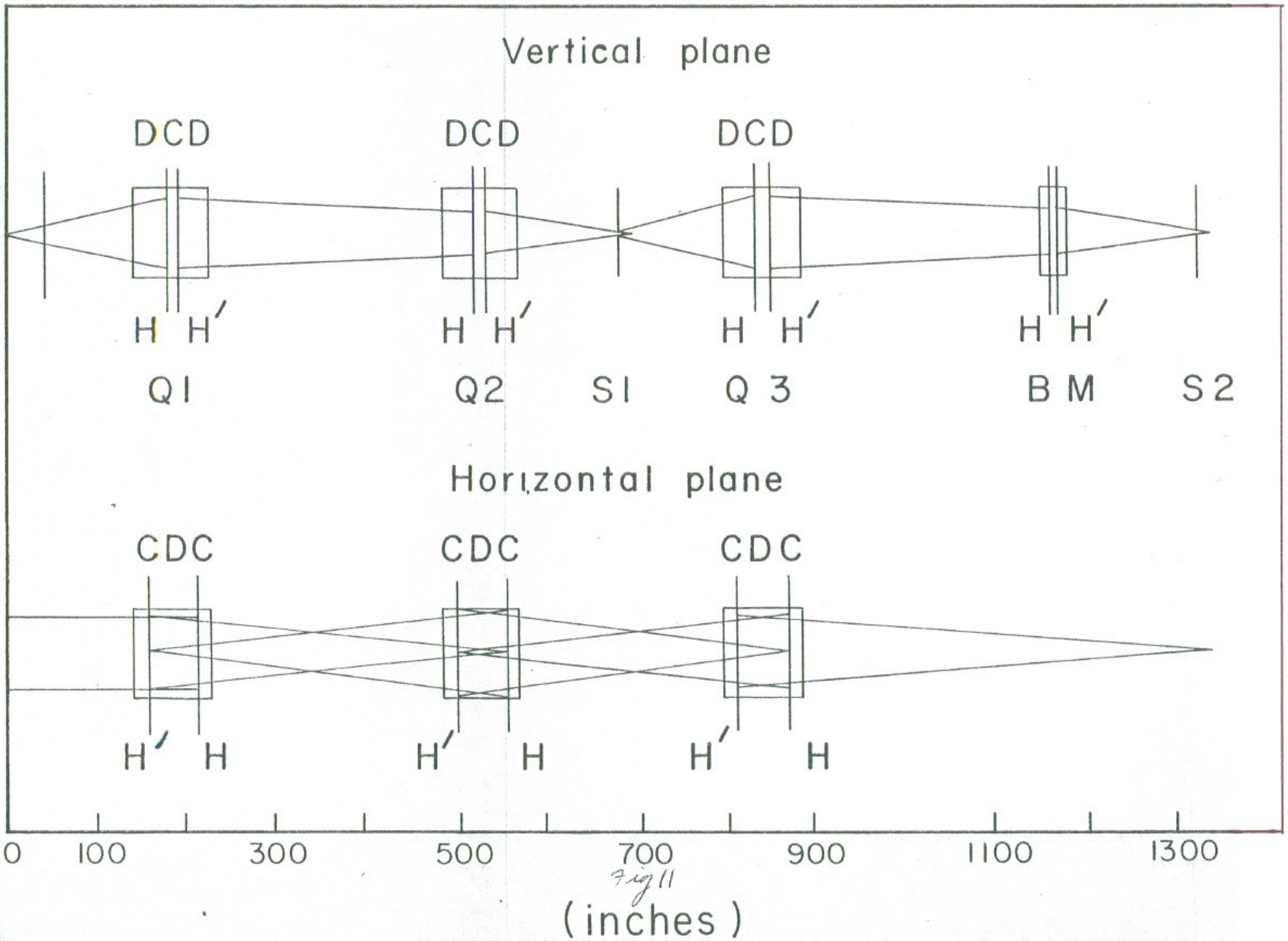
Vertical plane
DCD
DCD
DCD
H H'
H H'
H H'
H H'
Q1
Q2
S1
Q 3
B M
S 2
Horizontal plane
CDC
CDC
CDC
H' H
H' H
H' H
0
100
300
500
700
900
1100
1300
(inches)
Fig 11

Fig 11

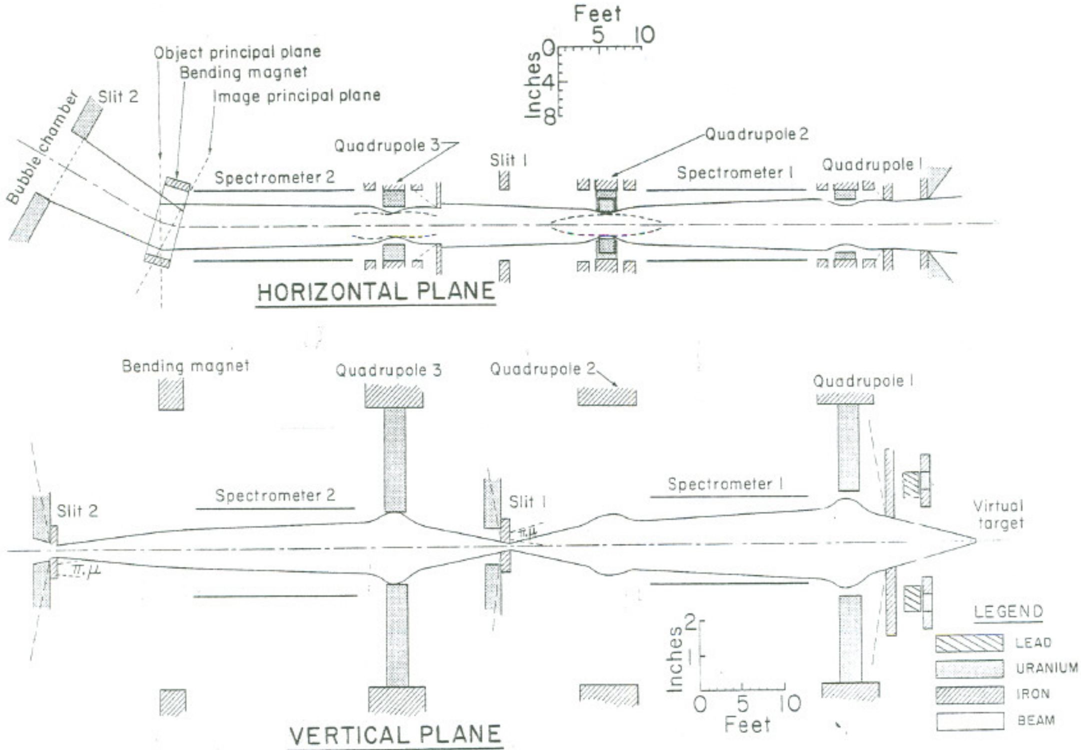

Feet
0
5
10
Inches
4
8
Object principal plane
Bending magnet
Image principal plane
Slit 2
Bubble chamber
Quadrupole 3
Slit 1
Quadrupole 2
Spectrometer 2
Spectrometer 1
Quadrupole 1
HORIZONTAL PLANE
Bending magnet
Quadrupole 3
Quadrupole 2
Quadrupole 1
Spectrometer 2
Spectrometer 1
Slit 2
Slit 1
Virtual target
Inches
2
1
0
5
10
Feet
LEGEND
LEAD
URANIUM
IRON
BEAM
VERTICAL PLANE

Fig. 12

0 0 1 0 0 3 0 3 9 0 2

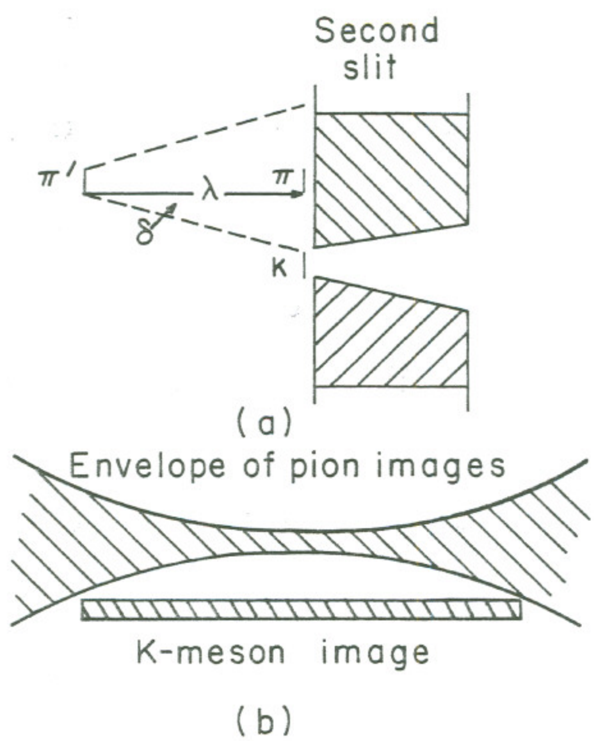

Fig. 13

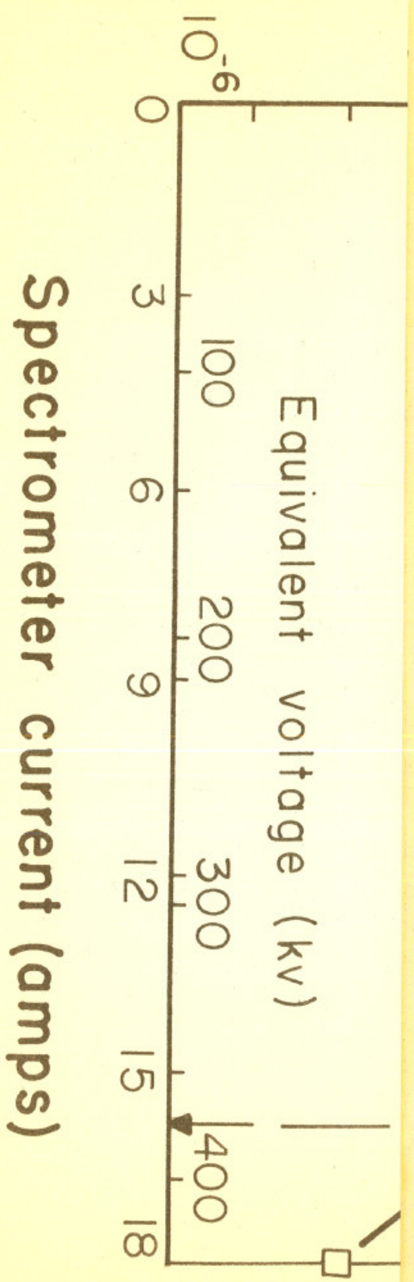

Fig 15

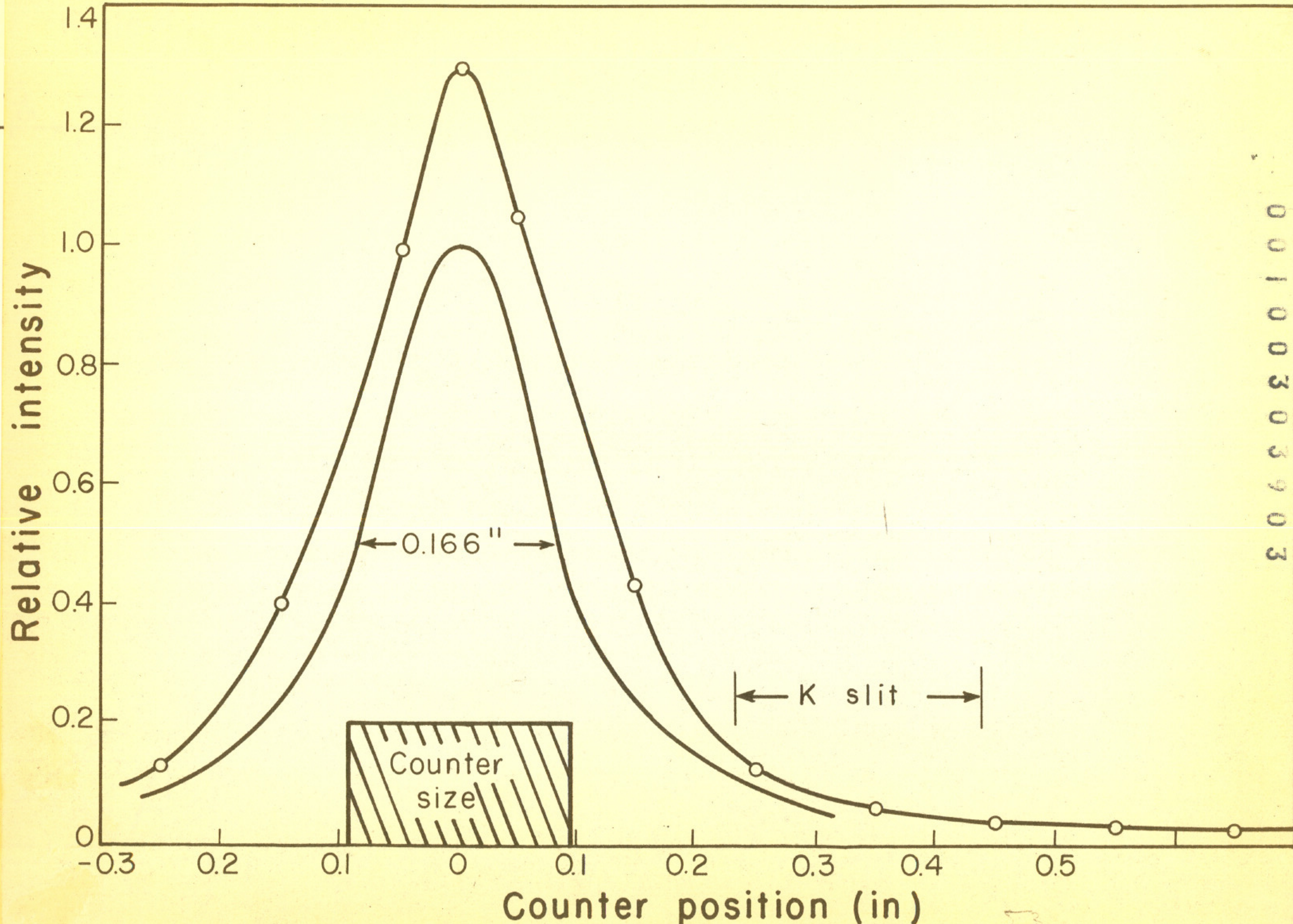

Fig 14

0010030 3903

55, #13-1

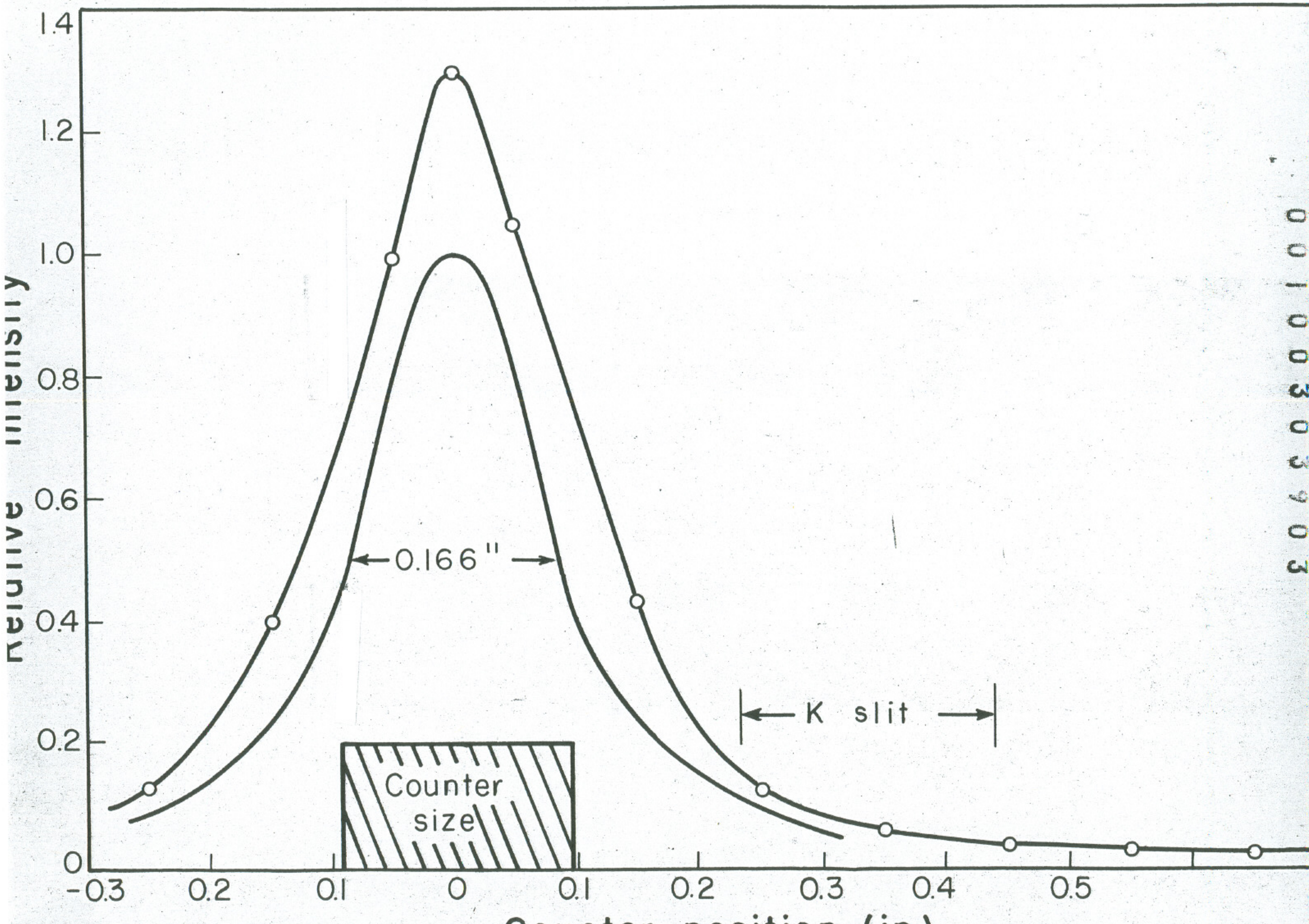

Fig 14

53

55 #13-1

0010030039003

0 0 1 0 0 3 0 3 9 0 4

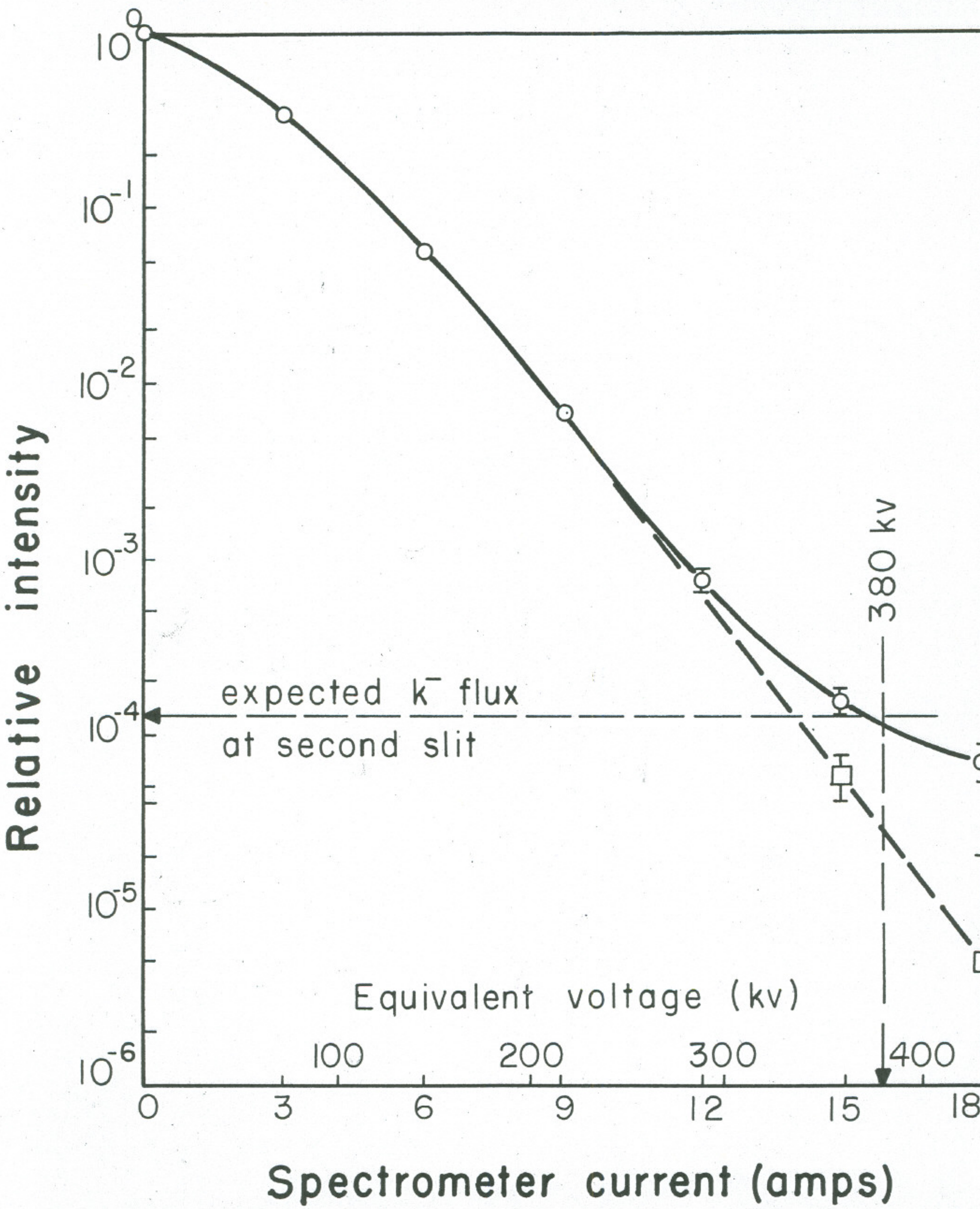

Fig 15

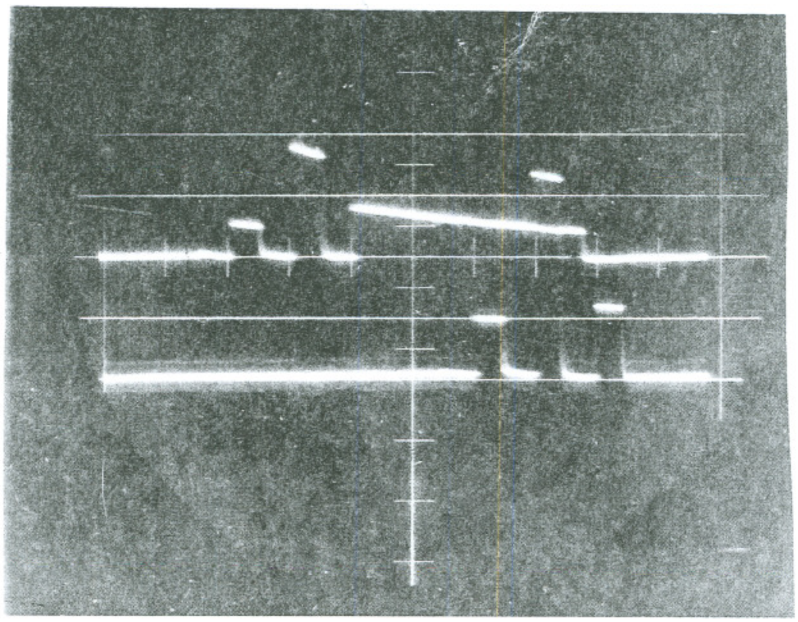

Fig. 16